System Identification for Three-dimensional AE-Tomography with Kalman Filter

Yoshikazu KOBAYASHI *, Tomoki SHIOTANI **, Kenichi ODA *
* Department of Civil Engineering, College of Science and Technology, Nihon University, 1-8-14, Kanda-Surugadai, Chiyoda-Ku, Tokyo, 101-8308, Japan
** Graduate School of Engineering, Kyoto University, Kyoto, Japan

Abstract. Three-dimensional AE-Tomography computes source locations of AE and reconstructs elastic wave velocity distribution simultaneously from arrival times of AE at receivers. Its algorithm is summarized that elastic wave velocity distribution is updated by using estimated travel times with conventional elastic wave velocity tomography technique. The estimated travel time is obtained as a difference between the arrival time and an estimated occurrence time at an estimated source location. The estimated occurrence time and source location are computed by using a source location technique that was proposed by the authors on presumed elastic wave velocity distribution. This fact implies that the reconstruction is executed with less boundary conditions than the conventional elastic wave velocity tomography because the travel times already involve "estimation" prior to the reconstruction. Hence, the accuracy of the reconstruction would be improved if observed travel times are added as its observations. Although the authors had adopted Simultaneous Iterative Reconstruction Technique (SIRT) for the reconstruction, this technique does not consider importance of each observation. Hence, less influence of an observation is consequently exerted on result of reconstruction even if the observation should play important role if large number of observations exist. Thus, in this paper, kalman filter is adopted as the reconstruction technique to properly control the weight of observations for reflecting its importance on the resultant elastic wave velocity distribution. The proposed method is verified by numerical investigations, and its applicability will be discussed.

1. Introduction

AE-Tomography is an identification problem that computes AE source locations and elastic wave velocity distribution by using travel times at receivers and locations of the receivers in two- and three-dimensional problems [1][2]. This technique was originally proposed by Schubert [3] with assumption of straight ray-path and conventional source location technique that uses the assumption of the straight ray-path to suppress rising of computational cost and make simplify the computational procedure. Although this technique suggested advantages of AE-tomography, it would be expected that accuracies of identified source locations and elastic wave velocity distribution would be degraded because of the assumption since the elastic velocity distributions are generally heterogeneous in real cases and the ray-paths normally curve on the heterogeneous velocity distribution as well known. In contrast, the technique that have been proposed by the authors considers the curve of the ray-paths on the basis of a ray-trace technique [4] in its entire algorithm, and a new source location technique that raises accuracies of the identification of the AE source locations was introduced as well.

On the reconstruction of the elastic wave velocity distribution, SIRT (Simultaneous Iterative Reconstruction Technique) has been adopted as an identification technique. This technique has been used for many of tomographic algorithm because its easiness of use whereas any a priori information cannot be in consideration. Furthermore, since SIRT emphasizes the difference of variables that are identified with its iterative procedure, it is sometimes difficult to assess state of convergence while the identification. Due to these facts, implementation of more advanced technique has been intended for the procedure of the identification. Thus, in this study, a new algorithm of AE-Tomography in which extended Kalimantan filter is adopted as the identification technique is introduced. Extended Kalimantan filter is an identification technique that considers a priori information as covariance matrices of observation errors and initial values for the variables that is identified between its true value, and, further, nonlinearity of observation equations. In following section, its methodology is introduced.

2. Methodology

AE-Tomography is a technique that computes source locations of AE and elastic wave velocity distribution simultaneously by using arrival times of AE at receivers and locations of the receivers. Figure 1 describes conceptual flow diagram of AE-Tomography. As described in Figure 1, an algorithm of AE-Tomography consists of two significant parts, one of the parts that is firstly conducted is to estimate the source location of AE, and another one that is secondary performed is to reconstruct the elastic wave velocity distribution. In both of the parts, curves of ray-paths that are caused by inhomogeneity of impedance are considered by using ray-trace technique. This ray-trace technique plays significant role in the algorithm of AE-Tomography, and its algorithm is briefly introduced in following subsection.

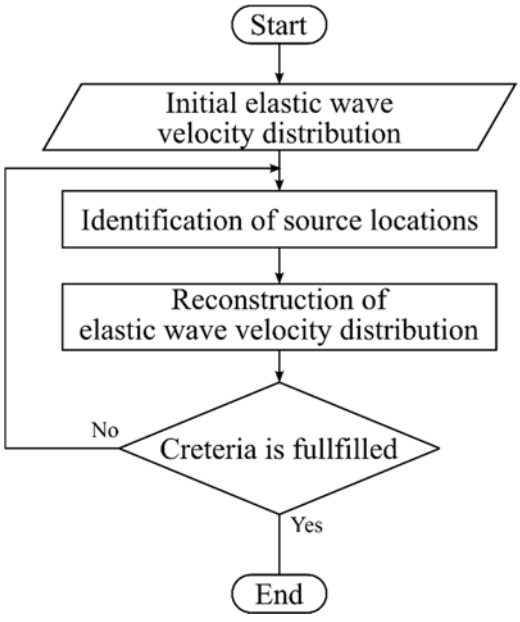

Figure 1 Conceptual flow diagram of AE-Tomography

2.1 Ray-trace technique

Ray-tracing is a technique that optimizes the ray-path to satisfy given conditions. In the elastic wave velocity tomography, a ray-path that gives minimum travel time from a source to a receiver is required since first travel times are generally used as observations to

reconstruct the elastic wave velocity distribution. For computing the optimized ray-path, volumes of interest is meshed by using hexahedral or tetrahedral cells. On the mesh, it is assumed that elastic wave velocity is constant in individual cells and ray-paths are drawn as polylines and individual nodes of the polylines exists at a nodal point of the mesh as illustrated in Figure 2. On these assumptions, the optimized ray-path is sought on the basis of Dijkstra's algorithm. In Dijkstra's algorithm, a graph that shows relationships between nodal points is generated by using weights that are identical to travel times between the nodal points in ray-tracing. Then, a shortest path from the source to the receiver is sought on the graph, and finally, the shortest path is adopted as the optimized ray-path. Thus, for ray-tracing, travel times between the nodal points are required, and it is computed as follows if the ray-path between the nodal points are assumed as straight lines.

$$T = \sum_i S_i l_i \tag{1}$$

in which, S_i is a slowness, a reciprocal of an elastic wave velocity, of cell i, and l_i is a length of a ray-path in cell i. Equation 1 indicates that computation of l_i is momentous for ray-tracing because S_i is normally presumed prior to performing it, and the computation is defined as calculation of intersection between a straight line and cell boundaries of the mesh because ray-path between the nodal points are presumed as straight lines and l_i is defined as a length of a segment that is a part of the ray-path and exists in cell i. Therefore, in this ray-trace technique, it is necessary to compute intersections of straight lines and hexahedral and tetrahedral cells. This is executed by using interpolate functions that are commonly used in Finite Element Analyses. For example, if a volume of interest is meshed by using hexahedral cells, it is not guaranteed that boundaries of the hexahedral cells are flat surface because a flat surface that involves four points does not exist in general. Thus, the boundary surfaces of the hexahedral cells are generally curved surfaces, and its influence must be considered in the computation of the intersections between the straight line and cell boundaries.

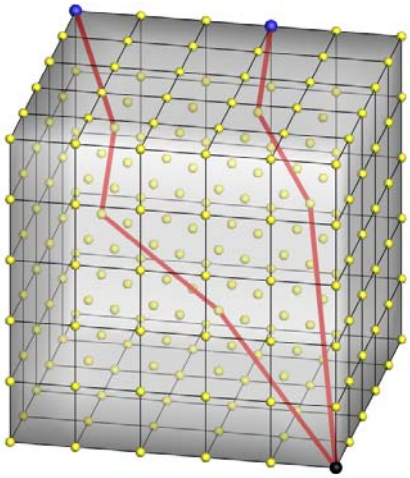

Figure 2 Examples of ray-paths in three-dimensional volume (Black sphere: source, Blue spheres: destination, Yellow spheres: nodal points, Red lines: ray-path)

On the other hand, any shape of hexahedral cells in global coordinate system are mapped on a rectangular-parallelepiped as illustrated in Figure 3. These mappings are described by using the interpolate functions as follows.

$$x = \sum_i N_i(\varepsilon, \eta, \xi) X_i$$

$$y = \sum_i N_i(\varepsilon, \eta, \xi) Y_i$$
$$z = \sum_i N_i(\varepsilon, \eta, \xi) Z_i \quad (2)$$

in which, N_i is a interpolate function that is associated with nodal point i, and ε, η, ξ are coordinates of a point in cell coordinate system and X_i, Y, Z_i are coordinates of nodal point i in global coordinate system. Since the straight line is described as an intersection of two planes, the straight line is described as follows in the cell coordinate system.

$$a_1 \sum_i N_i(\varepsilon, \eta, \xi) X_i + b_1 \sum_i N_i(\varepsilon, \eta, \xi) Y_i + c_1 \sum_i N_i(\varepsilon, \eta, \xi) Z_i + d_1 = 0$$
$$a_2 \sum_i N_i(\varepsilon, \eta, \xi) X_i + b_2 \sum_i N_i(\varepsilon, \eta, \xi) Y_i + c_2 \sum_i N_i(\varepsilon, \eta, \xi) Z_i + d_2 = 0 \quad (3)$$

Consequently, the coordinates of the intersections are obtained by substituting coordinates of cell boundaries in the cell coordinate system to Equation 3 in the cell coordinate system, and then, the coordinates of the intersections are given by mapping the coordinates in the cell coordinate system to the global coordinate system with Equation 2. Finally, l_i is computed by using the coordinates of the intersections in the global coordinate system.

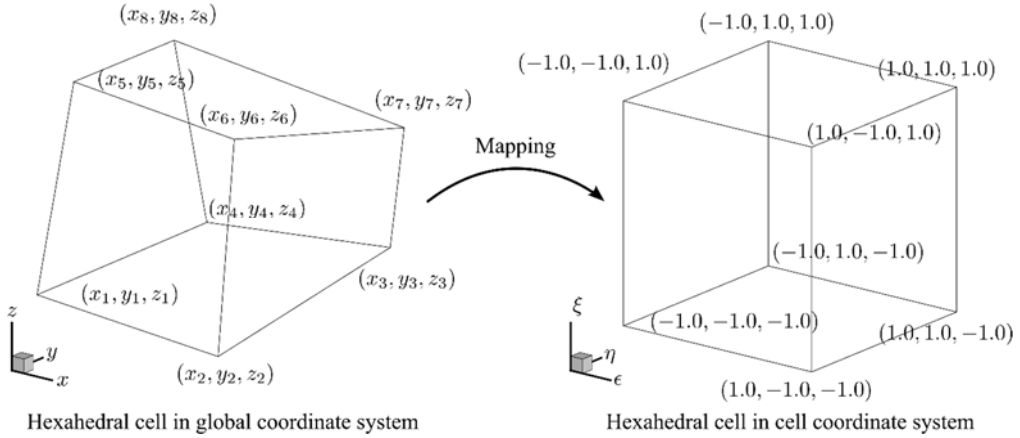

Figure 3 Mapping of hexahedral cells between global coordinate system and cell coordinate system

2.2 Source location technique

Estimations of the source locations of AE are conducted by using the ray-trace technique that was introduced in the previous section. Because the ray-tracing is executed on the three-dimensional mesh, the estimations of the source locations are conducted on the mesh as well. On the estimation of the source locations, firstly the ray-tracing is performed from individual receivers on the volume in every AE events. Due to this process, travel times from a receiver to all of the other nodal points are computed as follows.

$$O_{ijk} = A_{ik} - T_{ijk} \quad (4)$$

where A_{ik} is an arrival time of AE at receiver k in AE event i, T_{ijk} is a travel time from receiver k to nodal point j in AE event i and O_{ijk} is a potential occurrence time at nodal point j on receiver k in AE event i.This potential occurrence time implies that AE must be emitted at the potential occurrence time O_{ijk} from nodal point j if arrival time of AE at receiver k is observed as A_{ik} in AE event i. Thus, if n receivers are installed on the volume, individual nodal points has n potential occurrence times consequently in individual events. The potential occurrence times are identical to one another at a source location of the AE

event if resolution of the ray-path and elastic wave velocity distribution is infinitely precise by meshing the volume infinitely fine. Hence, the source location of the AE event can be find by seeking a nodal point at which the potential occurrence time is identical. However, it is generally impossible with regards to its computational cost, and normally the volume is meshed rougher than the infinitely precise one with consideration on balance between its benefit and cost. Therefore, in this study, the condition is relaxed and a nodal point that gives minimum variance of the occurrence times is chosen as the source location of AE event, and the variance of the occurrence time V_{ij} are shown as follows.

$$V_{ij} = \frac{\sum_k (O_{ijk} - \bar{O}_{ij})^2}{n} \tag{5}$$

in which

$$\bar{O}_{ij} = \frac{\sum_k O_{ijk}}{n} \tag{6}$$

It should be noted that the reconstruction of the elastic velocity distribution requires occurrence time of AE event in its algorithm as introduced in following section. The occurrence time is approximated by the average of the potential occurrence times $\bar{O}_{ij}$.

2.3 Reconstruction of elastic wave velocity distribution

The reconstruction of the elastic velocity distribution has been conducted by using a conventional algorithm that updates the distribution, for example, to minimize differences between observed and theoretical travel times at receivers in many cases. This approach is also adopted in the algorithm of AE-Tomography. In the algorithm of AE-Tomography, an arrival time at a receiver is described as follows.

$$T_{ik} = \sum_j S_j l_{ijk} + \bar{O}_i \tag{7}$$

in which, T_{ik} is an arrival time of AE at receiver k in AE event i, S_j is slowness of cell j, l_{ijk} is a length of a ray-path that from a source to receiver k in cell j on AE event i, and $\bar{O}_i$ is an occurrence time of the AE event i. In Equation 7, while the ray-path from the source to the receiver and the occurrence time of the AE event are used, the source information is generally unknown in observation of AE. Thus, in AE-Tomography, the source location technique is used for the estimation of the source location and the occurrence time of the AE event, and the ray-path is obtained by executing the ray-tracing from the estimated source location to the other nodal points. On these assumptions, Equation 7 is written as follows

$$\Delta T_{ik} = T_{ik} - \bar{O}_i = \sum_j S_j l_{ijk} \tag{8}$$

in which ΔT_{ik} is a first travel time. It should be noted that a ray-path that gives minimum travel time from the estimated source location to receiver k is chosen to compute l_{ijk}. This equation is identical to observation equation of conventional elastic wave velocity tomography. A difference between Equation 8 and the observation equation of the conventional elastic wave velocity tomography is computation of the first travel time that is shown in left side of Equation 8. In AE-Tomography, this term is shown as difference of the observed arrival time and estimated occurrence time of the AE event while it is immediately observed first travel time in the conventional elastic wave velocity tomography. This implies that the left hand of the observation equation that corresponds to the first travel time in the conventional elastic velocity tomography involves an estimated quantity in AE-Tomography, and its reliability is lower than the observed first travel time. This fact indicates that the accuracy of the reconstructed elastic wave velocity distribution in AE-Tomography is generally lower than the one that is computed by using the conventional elastic wave velocity tomography under same condition. However, costs of observations would be lower in

AE-Tomography than the elastic wave velocity tomography because the source information is not necessary, and consequently, it is possible to increase number of the observations. This characteristic would cover the disadvantage.

On the other hand, in identification techniques that are involved in a group of Kalman Filter, the system is written as follows.

$$x_{k+1} = x_k$$
$$y_k = H_k x_k + v_k \tag{9}$$

in which, x_k is a state vector at time k, y_k is a observation vector at time k, H_k is a observation matrix at time k, and v_k is a measurement noise vector at time k. It is noteworthy that the state vector x_k is assumed to be unchanged while the identification. It is noted that x_k and y_k correspond to a vector slowness of the individual cells and the first travel times that are estimated by using the arrival times and the estimated occurrence times. By rewriting Equation 8 to the form of Equation 9, the observation equation of AE-Tomography is described rewritten as follows.

$$\begin{Bmatrix} \Delta T_1 \\ \Delta T_2 \\ \vdots \\ \Delta T_n \end{Bmatrix} = \begin{bmatrix} l_{11} & l_{12} & \cdots & l_{1m} \\ l_{21} & l_{22} & \cdots & l_{2m} \\ \vdots & \vdots & \ddots & \vdots \\ l_{n1} & l_{n2} & \cdots & l_{nm} \end{bmatrix} \begin{Bmatrix} S_1 \\ S_2 \\ \vdots \\ S_n \end{Bmatrix} + \begin{Bmatrix} v_1 \\ v_2 \\ \vdots \\ v_n \end{Bmatrix} \tag{10}$$

It should be noted that Equation 10 is actually a nonlinear equation while it looks like a linear function because the ray-path would move with variation of the slowness vector x_k. Thus, Extended Kalman Filter is adopted as the identification technique in this paper. In the extended Kalman filter, the slowness vector x_k is updated on a process that is described as follows.

$$K_k = P_k H_k^T [H_k P_k H_k^T + R_k]^{-1} \tag{11}$$
$$x_k = x_{k-1} + K_k [y_k - H_k x_{k-1}] \tag{12}$$
$$P_k = (I - K_k H_k) P_{k-1} \tag{13}$$

in which, P_k is a covariance matrix of the state vector x_k, and R_k is a covariance matrix of the measurement noise v_k. It is noted that P_k and R_k indicates reliability of the state vector x_k and the observation vector y_k, respectively. On the reconstruction, firstly, K_k that is called Kalman Gain is computed by using Equation 11, then x_k is updated by using the Kalman gain with Equation 12. Finally, P_k is updated to consider the variation of the reliability of the state vector x_k by using Equation (13). This procedure is iteratively executed until a predefined criterion is fulfilled, and the resultant state vector x_k is adopted as the reconstructed slowness distribution.

3. Validation

The introduced algorithm is validated by performing a series of numerical investigations. Figure 4 Left shows a numerical model that is used for the investigations. The model is a cube with edges of 10m, and consists of two blocks, one is high velocity region which color is red and another is low velocity region which color is blue respectively in Figure 4 Left. In this model, it is assumed that eight receivers are installed at apexes of the volume and source locations of 20 AE events are randomly generated in the volume. Arrival times of the AE events at the receivers are computed by executing the ray-tracing from the individual generated source locations. It should be noted that the average of the arrival times at the receivers is 2.71E-3[s]. The computed arrival times at the receivers are used as observations for the reconstruction of elastic wave velocity distribution. Figure 4 Right shows an initial elastic wave velocity distribution. Homogeneous elastic wave velocity distribution is adopted as the initial distribution, and its elastic wave velocity is set to 4000 m/s. This initial

velocity distribution is updated by using the introduced algorithm with conditions that are listed as Case 1 to Case 4 in Table 1.

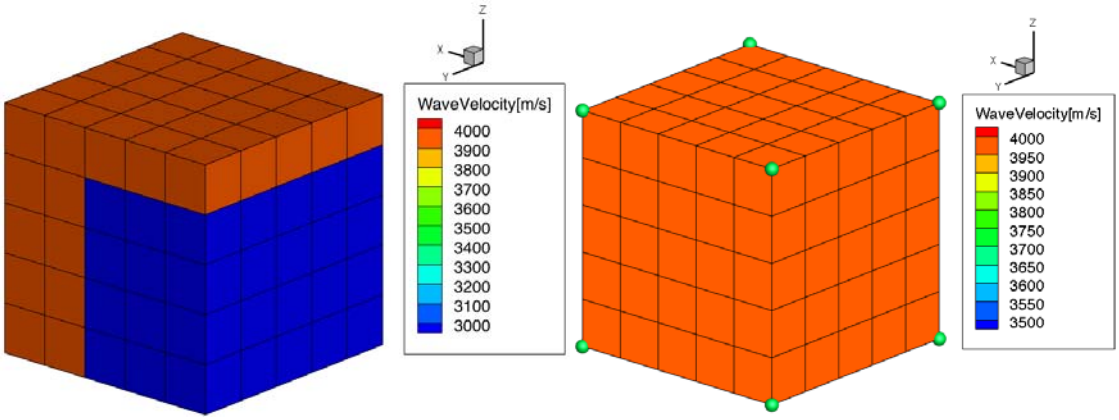

Figure 4 Target (Left) and initial (Right) elastic wave velocity distribution

Table 1 Diagonal terms of covariance matrix R_k and P_0

	Diagonal term of P_0	Diagonal term of R_k
Case 1	6.25E-10	1.00E-5
Case 2	6.25E-10	1.00E-6
Case 3	6.25E-10	1.00E-7
Case 4	6.25E-10	1.00E-8

In these cases, the reliability of the arrival times that are controlled by changing the diagonal term of the covariance matrix R_k with the artificially defined variances of the arrival times in Table 1 while the diagonal term of the P_0 that is initial matrix of P_k is set to 6.25E-10 of which square root corresponds to 10% of the slowness of the initial distribution. It should be noted that non-diagonal terms of the R_k and P_0 are set to zero since independence of x_k and v_k is assumed. Figure 5 shows the reconstructed elastic wave velocity distribution of Case 1 and 4. According to Figure 5, the reconstructed elastic wave velocity contour is closer in Case 4 to the target wave velocity distribution than Case 1. This is because the variance of the arrival times in Case 1 is relatively large in contrast with the average of the arrival times. If the average error of the arrival times can be approximated as square root of the variance, it is 3.16E-3 and it approximately 117 % of the average of the arrival times. This fact implies that all of the digits of the arrival times are unreliable, and consequently, influence of the observation equation to the reconstruction is limited. On the other hand, the error in Case 4 is very small to the average of the arrival times, and finally the arrival times are evaluated highly reliable. Thus, the elastic wave velocity distribution is updated to eliminate the difference between the observed and computed arrival times. Hence, the resultant velocity distribution is closer to the target one.

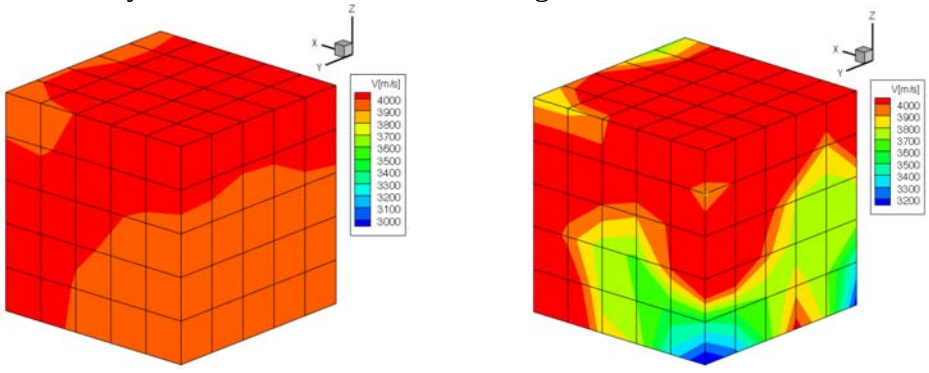

Figure 5 Reconstructed wave velocity distribution in Case1 (Left) and Case 4 (Right)

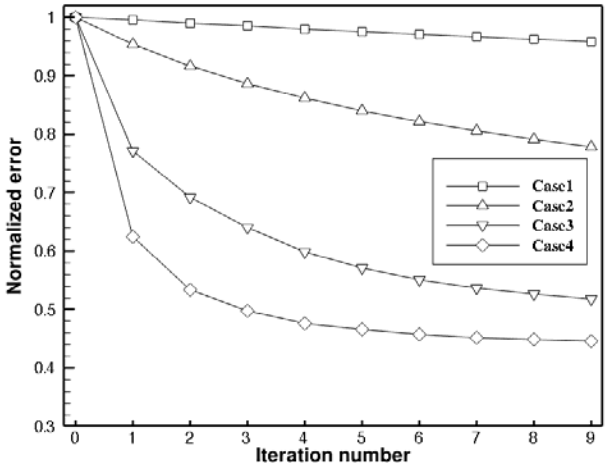

Figure 6 Relations between iteration number and normalized error

Figure 6 shows relations between the normalized error norm of the arrival times and iteration number. According to Figure 6, it is revealed that the normalized error is more reduced in case that the variance is set smaller. This also implies that the observed equation is considered significantly in the small variance cases. These facts reveals that the reliability of the arrival times can be controlled by setting adequate R_k. The diagonal terms of R_k can be set to each arrival time individually, and it enables to control the reliability of the each arrival time.

4. Conclusions

The algorithm of the three-dimensional AE-Tomography on the basis of extended kalman filter was introduced in this paper, and the method was validated by executing the numerical investigations. Based on the results, conclusions are drawn as follows.

1. We introduced the flow of the three-dimensional AE-Tomography algorithm that considers refraction and diffraction of pressure wave on the heterogeneous elastic wave velocity distribution on the basis of extended kalman filter.
2. The reconstructed elastic wave velocity distribution was closer to the target one in the cases that the smaller diagonal terms of R_k were set.
3. The normalized error of the arrival times was smaller in the cases that the smaller diagonal terms of R_k were set as well.
4. These facts suggest that the reliability of the arrival times can be controlled by giving adequate quantity to the diagonal term of R_k.

References

[1] Kobayashi, Y. and Shiotani, T., Seismic tomography with estimation of source location for concrete structures, Structural Faults and Repair 2012, 2012, Edinburgh

[2] Kobayashi, Y. and Shiotani, T., Oda, K., Three-dimensional AE-Tomography with accurate source location technique, Structural Faults and Repair 2014, 2014, London

[3] Schubert, F., “Tomography Techniques for Acoustic Emission Monitoring”, 9th European NDT Conference, 2006, Berlin.

[4] Kobayashi, Y., Mesh-independent ray-trace algorithm for concrete structures, Constructions and Building Materials, Volume 48, pp. 1309–1317, Elsevier, 2013.11